

---

# Sterically Stabilized Liposomes Labeled with Indium-111 to Image Focal Infection

Otto C. Boerman, Gert Storm, Wim J.G. Oyen, Louis van Bloois, Jos W.M. van der Meer, Roland A.M.J. Claessens, Daan J.A. Crommelin and Frans H.M. Corstens

*Departments of Nuclear Medicine and Internal Medicine, University Hospital, Nijmegen, The Netherlands; and Department of Pharmaceutics, Utrecht Institute for Pharmaceutical Sciences, University of Utrecht, Utrecht, The Netherlands*

---

To determine the potential of sterically stabilized liposomes to image infectious and inflammatory foci, the *in vivo* behavior of <sup>111</sup>In-labeled PEGylated (coated with polyethylene glycol) liposomes was studied in a rat model. **Methods:** Indium-111-PEGylated liposomes were administered intravenously to rats infected with *S. aureus* in the left calf muscle. The distribution of the radiolabel was studied by gamma counting of dissected tissues and gamma camera imaging for 48 hr. As a reference agent, the preparation of <sup>111</sup>In-IgG was included in these studies. **Results:** Clearance of the PEGylated liposomes from the blood compartment was similar to the clearance of <sup>111</sup>In-IgG in this model ( $t_{1/2} \approx 20$  hr). Uptake of the radiolabel in the abscess with the <sup>111</sup>In-liposomes was twice as high as the uptake following injection of <sup>111</sup>In-IgG (2.7 %ID/g versus 1.1 %ID/g at 48 hr postinjection). Tissue counting revealed that abscess-to-muscle ratios reached values up to 20 and 34 (24 and 48 p.i., respectively). As early as 1 hr postinjection, the abscess could be visualized scintigraphically. **Conclusion:** The *in vivo* characteristics of this liposomal formulation in this rat model indicate that sterically stabilized liposomes labeled with gamma emitters might be a valuable addition to the arsenal of radiopharmaceuticals currently used for infection imaging.

**Key Words:** indium-111-PEGylated liposomes; sterically stabilized liposomes; infection imaging

**J Nucl Med 1995; 36:1639-1644**

---

**L**ocalization of infectious and inflammatory lesions is a challenging goal in nuclear medicine, as it may have important implications for the management of patients. Over the last two decades, numerous radiopharmaceuticals have been developed and clinically investigated. Each of these techniques, although successful in many cases, has its particular disadvantages (1,2). Recently, we formulated characteristics of the ideal radiopharmaceutical for the detection of sites of infection and inflammation (3). In view of the limitations of each of the conventional radiopharma-

ceuticals, there is a continued search for safe agents that will rapidly visualize foci of infection and inflammation with high degrees of sensitivity and specificity.

Liposomes are microscopic lipid vesicles consisting of one or more concentric lipid bilayers enclosing discrete aqueous spaces. Liposomes have been investigated extensively as carriers for drugs in attempts to achieve selective deposition and/or reduced toxicity (4-6). Liposomes, as formulated in the past, are rapidly taken up by cells of the mononuclear phagocyte system (MPS), primarily those located in the liver and spleen. This natural targeting could be heightened by increasing the vesicle size and/or including negatively charged lipids (e.g., phosphatidylserine) into the bilayers. Enhanced efficacy of macrophage-activating factors and drugs directed against pathogens residing within MPS cells of the liver and spleen has clearly been demonstrated (7,8). Due to their rapid association with MPS cells, however, liposomes showed inefficient targeting to other tissues *in vivo*. In recent years, the development of new formulations of long-circulating liposomes (also referred to as Stealth\* or sterically stabilized liposomes) has greatly broadened the potential applications of liposomes for targeted delivery. Because sterically stabilized liposomes show reduced uptake by MPS cells, and as a consequence, prolonged circulation times, the opportunity for targeting to other tissues is enhanced. The recent observations with these novel liposomes showing enhanced localization in tumors (9,10) and sites of infection (11,12) confirm the improved outlook for targeted liposomal delivery. At present, small (about 100 nm or less) liposomes containing hydrophilic phosphatidylethanolamine (PE) derivatives of polyethylene glycol (PEG) appear to show the best performance in terms of prolonged circulation and reduced MPS uptake as compared to other long-circulating liposomes (13).

Conventional liposomes labeled with gamma-emitting radionuclides have been used successfully for scintigraphic imaging of infection (14) and inflammation (15-17). We hypothesized that reduced MPS uptake of sterically stabi-

---

Received Aug. 17, 1994; revision accepted Jan. 9, 1995.

For correspondence or reprints contact: O.C. Boerman, MD, Department of Nuclear Medicine, University Hospital Nijmegen, P.O. Box 9101, 6500 HB Nijmegen, The Netherlands.

\*Stealth liposomes is a registered trademark name of Liposome Technology, Inc., Menlo Park, CA.

lized liposomes will improve their localization in the infectious focus. Therefore, we studied the biodistribution of  $^{111}\text{In}$ -labeled PEGylated liposomes in rats with focal *S. aureus* infections. The preparation of  $^{111}\text{In}$ -IgG was included in these studies as a reference to estimate the clinical potential of PEGylated liposomes as an imaging agent.

## MATERIALS AND METHODS

### Liposome Preparation

Partially hydrogenated egg-phosphatidylcholine with an iodine value of 40 (PHEPC) was prepared as previously described (18). The polyethyleneglycol (PEG) 1900 derivative of distearoylphosphatidyl-ethanolamine (PEG-DSPE) also was prepared as previously described (19).

A lipid mixture in chloroform/methanol (10/1, v/v) was prepared with the mole ratio composition of 0.15:1.85:1 (PEG-DSPE/PHEPC/cholesterol). A lipid film was formed by rotary evaporation followed by high vacuum to remove residual organic solvent. The lipids were dispersed at room temperature in 6 mM Desferal in 0.9% HEPES buffer (10 mM HEPES, 135 mM NaCl, pH 7.5) at an initial phospholipid concentration of 120 mM. The resultant multilamellar vesicles were sized by bath sonication for 2 hr. Untrapped deferoxamine mesylate (Desferal) was removed by cation exchange resin Dowex 50WX4 (20). The particle size distribution was determined by dynamic light scattering. The liposomes had a mean size of 90–100 nm.

### Labeling Procedures

Preformed Desferal containing liposomes were labeled with  $^{111}\text{In}$  essentially as previously described (12,21). Indium-111 was transported by hydroxyquinoline (oxine) through the bilayer and trapped irreversibly in the internal aqueous phase by the encapsulated Desferal. Briefly, the liposomes (75  $\mu\text{mole}$  phospholipid/ml) were incubated for 1 hr at room temperature with 2–3  $\mu\text{Ci}$   $^{111}\text{In}$ -oxine per  $\mu\text{mole}$  phospholipid. Unencapsulated  $^{111}\text{In}$ -oxine was removed by gel filtration on a 10DG Econo Pak column (Bio-Rad, Richmond, CA). More than 75% of the  $^{111}\text{In}$  label was entrapped within the liposomes.

Human, nonspecific polyclonal IgG was conjugated to diethylenetriaminepentaacetic bicyclic anhydride (bicyclic DTPA) according to the method described by Hnatowich et al. (22) and labeled with  $^{111}\text{In}$ . Labeling efficiency as determined by ITLC was higher than 95%.

### Animal Model

A calf muscle abscess was induced in young, male, randomly bred Wistar rats (weight 200–220 g). After ether anesthesia, approximately  $2 \times 10^8$  colony forming units of *S. aureus* in 0.1 ml 50:50% suspension of autologous blood and normal saline were injected in the left calf muscle (23). Twenty-four hours after the inoculation, when swelling of the muscle was apparent, the respective radiopharmaceuticals were injected through the tail vein.

### Biodistribution Studies

Twenty-four hours after *S. aureus* inoculation, 30 rats were divided randomly into two groups. One group of 15 rats was injected with 400 kBq  $^{111}\text{In}$ -liposomes through the tail vein. As a control, the other group of rats received 400 kBq ( $=25 \mu\text{g}$ )  $^{111}\text{In}$ -IgG.

At 2, 24 and 48 hr postinjection, five rats in each group were killed with 30 mg intraperitoneally injected phenobarbital. Blood was obtained by cardiac puncture. Following cervical dislocation,

several tissue samples (infected left calf muscle, right calf muscle, liver, spleen, kidney, intestine, right femur and bone marrow from the right femur) were dissected, weighed and their activity was measured in a shielded well-type gamma counter. To correct for physical decay and to calculate radiopharmaceuticals uptake in each organ as a fraction of the injected dose, aliquots of the injected dose were counted simultaneously.

### Imaging Protocol

*S. aureus* infection was induced in another six rats as described above. Twenty-four hours later, three rats received 4 MBq  $^{111}\text{In}$ -liposomes through the tail vein. For comparison, the other three rats received 4 MBq  $^{111}\text{In}$ -IgG. Rats were anesthetized (halothane/nitrous oxide) and were placed prone on a single-head gamma camera equipped with a parallel-hole, medium-energy collimator. The two groups of rats were imaged synchronously at 5 min, 0.5, 1, 2, 4, 6, 24 and 48 hr postinjection. Symmetric 20% windows were used for both the 173- and 247-keV energy peaks. Images (300,000 cts/image) were obtained and stored in a  $256 \times 256$  matrix. After 48 hr, the animals were killed and dissected to determine the biodistribution of the radiolabel.

The scintigraphic results were analyzed by drawing regions of interest over the abscess, the normal contralateral calf muscle, used as a background region, and over the whole animal. Abscess-to-background ratios and the percentage of residual activity in the abscess (abscess-to-whole body ratio) were calculated.

### Statistical Analysis

All mean values are given  $\pm 1$  s.d. Statistical analysis was performed using the unpaired two-tailed Student's t-test.

## RESULTS

The biodistribution of  $^{111}\text{In}$ -labeled PEGylated liposomes and  $^{111}\text{In}$ -IgG in rats with *S. aureus* infections are shown in Table 1. Blood levels of  $^{111}\text{In}$  following injection of both radiopharmaceuticals were similar. Localization in the abscess increased over the time course of the experiment, from 0.7% ID/g at 2 hr postinjection to 2.7% ID/g at 48 hr postinjection. Both the increase over the 2–24-hr period ( $p < 0.002$ ) as well as the increase over the 24–48-hr ( $p < 0.03$ ) were statistically significant. Abscess uptake of the  $^{111}\text{In}$ -liposomes was approximately twice as high as  $^{111}\text{In}$ -IgG uptake (24 and 48 hr postinjection,  $p < 0.005$ ).

Besides accumulation in the abscess, a marked accretion of the liposomal radiolabel was observed in the spleen over the 48-hr time period. Mean uptake rose to 16% ID/g at 48 hr, indicating that almost 10% of the injected dose accumulated in the spleen. The liver, which together with the spleen is the major organ with mononuclear phagocytic activity, showed less pronounced accumulation; during the last 24 hr of the experiment, there was a slight but significant increase of  $^{111}\text{In}$  activity in the liver (from 0.9% to 1.4% ID/g;  $p < 0.003$ ). Separate measurement of the activity in the right femur and the bone marrow indicated an increase of activity in the bone marrow as well (from 1.2% to 2.0% ID/g;  $p < 0.005$ ). All other tissue samples examined had low activity levels which decreased with time. Except for the spleen, the abscess was the tissue with the highest activity from 24 hr onwards.

**TABLE 1**  
Biodistribution of Indium-111-PEGylated Liposomes and Indium-111-IgG in Rats with *S. aureus* Infections in Calf Muscle (%ID/g  $\pm$  s.d.)

Organ	2 hr p.i.		24 hr p.i.		48 hr p.i.	
	Liposomes	IgG	Liposomes	IgG	Liposomes	IgG
Blood	4.45 $\pm$ 0.26	3.75 $\pm$ 0.15	2.00 $\pm$ 0.06	1.30 $\pm$ 0.1	0.84 $\pm$ 0.13	0.95 $\pm$ 0.15
Muscle	0.10 $\pm$ 0.04	0.13 $\pm$ 0.03	0.10 $\pm$ 0.01	0.15 $\pm$ 0.02	0.09 $\pm$ 0.02	0.15 $\pm$ 0.01
Abscess	0.73 $\pm$ 0.16	1.10 $\pm$ 0.14	1.93 $\pm$ 0.54	0.97 $\pm$ 0.04	2.73 $\pm$ 0.38	1.10 $\pm$ 0.09
Bone marrow	1.19 $\pm$ 0.20	1.54 $\pm$ 0.13	1.58 $\pm$ 0.29	1.30 $\pm$ 0.08	2.04 $\pm$ 0.46	1.11 $\pm$ 0.06
Bone	0.30 $\pm$ 0.09	0.56 $\pm$ 0.08	0.38 $\pm$ 0.13	0.35 $\pm$ 0.03	0.29 $\pm$ 0.17	0.33 $\pm$ 0.04
Lung	1.18 $\pm$ 0.21	1.12 $\pm$ 0.14	0.64 $\pm$ 0.07	0.54 $\pm$ 0.05	0.51 $\pm$ 0.34	0.42 $\pm$ 0.03
Spleen	4.32 $\pm$ 0.51	1.26 $\pm$ 0.53	11.66 $\pm$ 0.98	1.56 $\pm$ 0.19	16.12 $\pm$ 4.07	1.37 $\pm$ 0.11
Kidney	1.11 $\pm$ 0.16	4.40 $\pm$ 0.16	0.84 $\pm$ 0.07	4.78 $\pm$ 0.34	0.71 $\pm$ 0.10	4.57 $\pm$ 0.24
Liver	1.27 $\pm$ 0.41	1.40 $\pm$ 0.10	0.89 $\pm$ 0.14	1.11 $\pm$ 0.10	1.44 $\pm$ 0.24	1.10 $\pm$ 0.07
Small intestine	0.42 $\pm$ 0.08	0.38 $\pm$ 0.04	0.65 $\pm$ 0.09	0.23 $\pm$ 0.03	0.80 $\pm$ 0.12	0.21 $\pm$ 0.02

The abscess-to-muscle ratios are shown in Figure 1A. After injection of  $^{111}\text{In}$ -liposomes, this ratio increased steadily from 7.9 at 2 hr postinjection to 33.9 at 48 hr postinjection. Both the increase over the 2–24-hr time period ( $p < 0.013$ ) and the increase over the 24–48-hr time period ( $p < 0.011$ ) were statistically significant. Due to increasing activity in the abscess and decreasing activity in the blood, abscess-to-blood ratios also continued to increase up to 3.3 at 48 hr postinjection (Fig. 1B). The abscess-to-muscle ratios as well as the abscess-to-blood ratios 24 and 48 hr postinjection were significantly higher than those obtained with  $^{111}\text{In}$ -IgG ( $p < 0.02$ ).

The distribution of  $^{111}\text{In}$ -liposomes was also studied scintigraphically. The acquired images were compared with the  $^{111}\text{In}$ -IgG images. With  $^{111}\text{In}$ -liposomes, the abscess was visualized within 1 hr postinjection (Fig. 2).

Contrast between the infectious focus and the background improved with time. Besides high uptake in the abscess, marked localization was also observed in the spleen, which correlates with the biodistribution data. Quantification of the counts within the regions of interest, the abscess and the contralateral muscle indicated that the abscess-to-background ratio increased up to a value of 15.5 (Fig. 3A). In comparison to  $^{111}\text{In}$ -IgG abscess-to-background ratios, the ratios obtained with liposomes were significantly higher ( $p < 0.04$ ) from 4 hr postinjection onwards. The residual activity in the abscess (expressed as the percentage of the whole-body activity) also increased during the experiment (up to 18% at 48 hr postinjection) (Fig. 3B). From 24 hr onwards, the percentage residual activity in the abscess for  $^{111}\text{In}$ -liposomes was significantly higher than for  $^{111}\text{In}$ -IgG ( $p < 0.04$ ) (Fig. 3B). Indium-111-liposomes and  $^{111}\text{In}$ -IgG

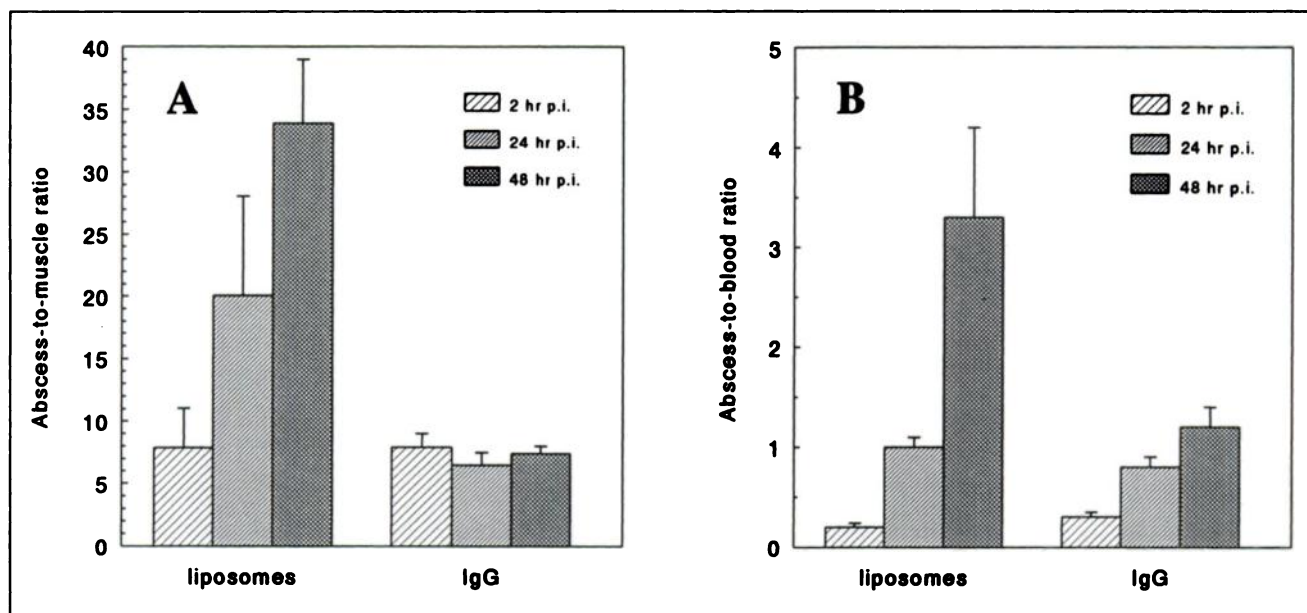


**FIGURE 1.** Abscess-to-muscle ratios (A) and abscess-to-blood ratios (B) at 2 hr, 24 hr and 48 hr postinjection for  $^{111}\text{In}$ -labeled PEGylated liposomes and  $^{111}\text{In}$ -IgG. The biodistribution data of five rats per time point were used. Error bars represent standard deviations.

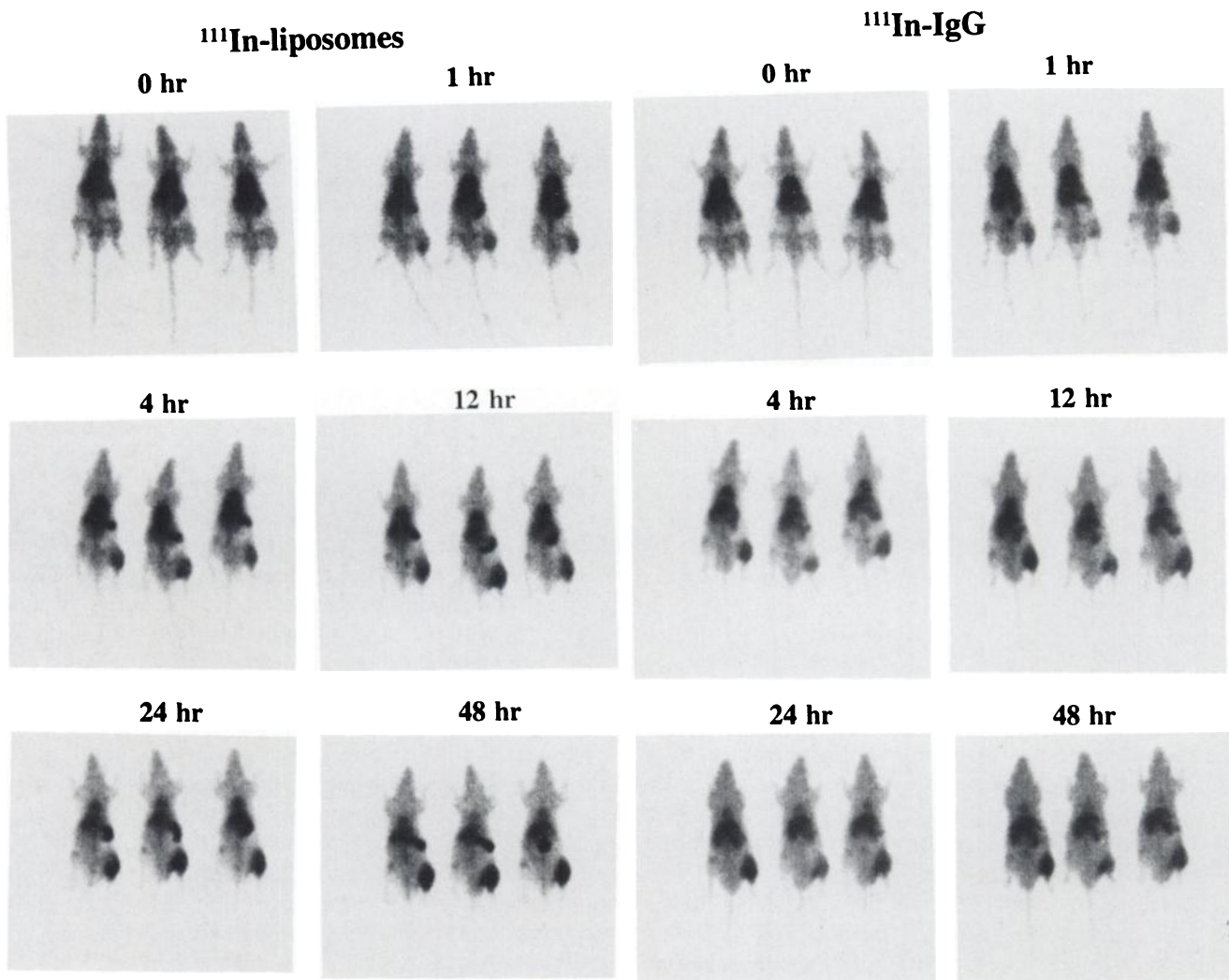


**FIGURE 2.** Scintigrams of rats with unilateral *S. aureus* infections in calf muscle imaged 0 hr (=5 min), 1 hr, 4 hr, 12 hr, 24 hr and 48 hr postinjection of  $^{111}\text{In}$ -labeled PEGylated liposomes (left) and  $^{111}\text{In}$ -IgG (right).

were eliminated from the blood compartment at a similar rate: 50% of the activity was still circulating 20 hr postinjection. In fact, during the distribution phase ( $t_{1/2\alpha}$ ) clearance of the  $^{111}\text{In}$ -liposomes appeared to be slower, while the elimination rate ( $t_{1/2\beta}$ ) of the liposomes was faster (Fig. 3C). Whole-body clearance of the  $^{111}\text{In}$  for liposomes and IgG was minimal: over the 48-hr time interval less than 5% of the injected dose was excreted.

## DISCUSSION

Sterically stabilized liposomes have been shown to localize preferentially in infectious foci (11,12) and radiolabeling with gamma emitters might be useful tools for imaging infectious and inflammatory foci. In this study, we evaluated the potential of  $^{111}\text{In}$ -labeled sterically stabilized liposomes to image bacterial infections of the left calf muscle in rats.

Clearance of  $^{111}\text{In}$ -labeled PEGylated liposomes from the blood was similar to  $^{111}\text{In}$ -IgG clearance in this model

( $t_{1/2} \approx 20$  hr), allowing sufficient abscess uptake. The PEGylated liposomes showed preferential localization in the infected calf muscle. Recently, PEGylated liposomes labeled with  $^{99\text{m}}\text{Tc}$  have been proposed as a blood-pool marker in nuclear medicine (24). In a study of rabbits, Tilcock et al. (24) found that the half-life of  $^{99\text{m}}\text{Tc}$ -PEG-liposomes in the circulation was 5–10 hr. Although it is difficult to compare blood circulation times in different animal species, PEGylated liposomes apparently clear somewhat faster from the circulation, which might be due to the larger size ( $\pm 200$  nm) of the vesicles used. Recently, Goins et al. tested  $^{99\text{m}}\text{Tc}$ -liposomes (mean size 185 nm) in rats with *S. aureus* infections (25). Their abscess-to-muscle ratios were high and in the same range as those reported in our study. In the Goins et al. study, however, urinary excretion amounted to 30% ID (as compared to <5% ID in our study), indicating that the non-PEGylated liposomes were less stable in vivo. In addition, the liposomal formulation in the Goins study displayed an even higher splenic

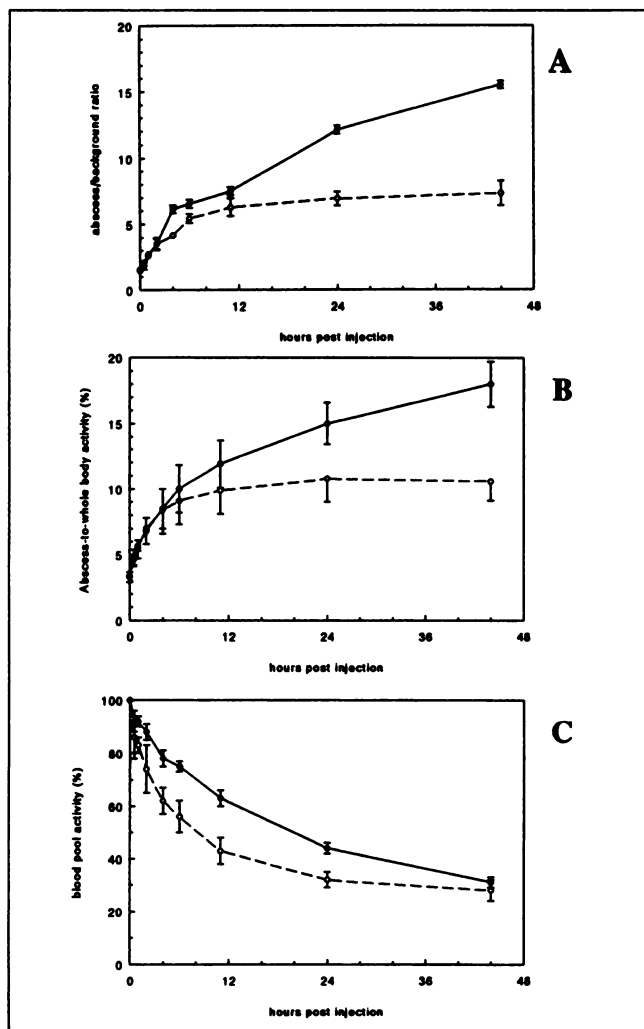


**FIGURE 3.** Quantitative analysis of the scintigraphic images of rats (three rats per group) injected with  $^{111}\text{In}$ -liposomes (●) and  $^{111}\text{In}$ -IgG (○). Abscess-to-background ratios (A), retained activity in the abscess as percentage of residual whole-body activity (B) and activity in the blood-pool region (C) were determined for both agents. Blood-pool activity measured 5 min postinjection was set at 100%. Error bars represent standard deviations.

accumulation (up to 39% ID/g). Obviously, in clinical practice,  $^{99\text{m}}\text{Tc}$  is preferable to  $^{111}\text{In}$ . We are conducting further studies to evaluate the characteristics of our liposomal formulation labeled with  $^{99\text{m}}\text{Tc}$ .

The mechanism of abscess accumulation of PEGylated liposomes has not been studied. Liposomes probably extravasate in areas of inflammation as a result of locally increased capillary permeability or through damaged endothelial linings. Several studies have clearly demonstrated that liposomes are able to exploit this phenomenon of locally increased microvascular permeability to an increasing extent when the residence time in the blood is extended (12,26). Since other investigators have shown that the uptake of long-circulating PEGylated liposomes by monocytes is insignificant (27,28), the role of inflammatory cells in the extravasation of these liposomes is not expected to be of considerable importance. Studies in other infection

and/or inflammation models could indicate the importance of the presence of bacteria, phagocytotic cells, enhanced vascular permeability, etc.

*S. aureus* bacteria were chosen as the infectious agent because they provide reproducible focal infections in rats. Other groups have used *E. coli* as the infectious agent. Highly similar results have been obtained in both models with  $^{111}\text{In}$ -IgG (29). How these radiolabeled liposomes localize other infections or inflammations remains to be determined, but the answer could reveal important information on the factors that determine liposomal accumulation.

Besides accumulation in the abscess, relatively high uptake was also observed in the spleen. Uptake in the other nontarget organs was relatively low and decreased with time. Consequently, target-to-background ratios steadily increased during the 48-hr time interval after injection. Based on tissue counting, abscess-to-muscle ratios were approximately four times higher than those obtained with  $^{111}\text{In}$ -IgG in this model. Biodistribution data as well as scintigraphic results indicate that  $^{111}\text{In}$ -liposomes have favorable imaging characteristics as compared to  $^{111}\text{In}$ -IgG, mainly because the absolute uptake in the abscesses 1 and 2 days postinjection was more than twice as high.

One of the most striking characteristics of  $^{111}\text{In}$ -labeled PEGylated liposomes in this model was the almost complete absence of kidney uptake (less than 1 %ID/g), resulting in high abscess-to-kidney ratios. With  $^{111}\text{In}$ -IgG, kidney activity exceeded 4% ID/g throughout the 48-hr time interval in this model. In patients, abdominal abscess localization with  $^{111}\text{In}$ -IgG is hampered by the relatively high renal uptake (30). The reduced kidney uptake obtained with  $^{111}\text{In}$ -liposomes cannot be explained by the low whole-body excretion because the same uptake was also observed with  $^{111}\text{In}$ -IgG. One might assume that the  $^{111}\text{In}$  label remains associated with Desferal after release from the liposomes, resulting in rapid clearance to the urine without glomer retention of the radiolabel.

The abscess-to-blood ratios obtained with  $^{111}\text{In}$ -liposomes were also much higher than those obtained with  $^{111}\text{In}$ -IgG (3.3 versus 1.0 at 48 hr). Based on this favorable characteristic one might expect that PEGylated liposomes, like radiolabeled autologous leukocytes, may be used to image vascular lesions.

We believe that liposomes have two major advantages over radiolabeled leukocytes: (a) they are readily available because liposomes can be easily and rapidly reconstituted from their lyophilized form (31) and (b) liposomes will not contain blood-derived infectious agents (e.g., HBV, HIV).

A disadvantage of  $^{111}\text{In}$ -liposomes imaging is high uptake in the spleen. High splenic uptake was also found in other preclinical studies using PEGylated liposomes (12,29). As observed with  $^{111}\text{In}$ -labeled autologous leukocytes, the spleen will most likely be the organ that receives the highest radiation burden when  $^{111}\text{In}$ -liposomes are used for infection imaging (32). This uptake, however, hardly limits the clinical efficacy of  $^{111}\text{In}$ -leukocytes (33). Hope-

fully, this also holds true for radiolabeled PEGylated liposomes.

## CONCLUSION

The ideal universal radiopharmaceutical for infection and inflammation imaging does not exist. Our results indicate that labeled PEGylated liposomes have attractive biodistribution and imaging characteristics, and further clinical evaluation is warranted.

## ACKNOWLEDGMENTS

The skilled assistance of G. Grutters in the animals experiments and E. Koenders in the preparation of the radiopharmaceuticals is gratefully appreciated. The authors thank Liposomes Technology, Inc. for supplying the polyethyleneglycol.

## REFERENCES

1. Datz FL. The current status of radionuclide infection imaging. In: Freeman LM, ed. *Nuclear medicine annual 1993*. New York: Raven Press; 1993:47-75.
2. Corstens FHM, Oyen WJG, Becker WS. Radioimmunoconjugates in the detection of infection and inflammation. *Semin Nucl Med* 1993;23:148-164.
3. Corstens FHM, Van der Meer JWM. Chemotactic peptides: new locomotion for imaging of infection? *J Nucl Med* 1991;32:491-494.
4. Gregoriadis G, ed. *Liposome technology*, vol. 3. Boca Raton, FL: CRC Press; 1993.
5. Nässander UK, Storm G, Peeters PAM, Crommelin DJA. Liposomes. In: Chasin M, Langer R, eds. *Biodegradable polymers as drug delivery systems*. New York: Marcel Dekker; 1990:261-338.
6. Crommelin DJA, Schreier H. Liposomes. In: Kreuter J, ed. *Colloidal drug delivery systems*. New York: Marcel Dekker Inc.; 1994:73-89.
7. Bakker-Woudenberg IAJM, Roerdink FH, Scherphof GL. Drug targeting in antimicrobial chemotherapy by means of liposomes. In: Gregoriadis G, ed. *Drug carriers. Trends and progress*. Chichester, UK: Wiley; 1988:325-336.
8. Juliano RL. Liposomes as drug carriers in the therapy of infectious diseases. In: Roerdink FHD, Kroon AM, eds. *Drug carrier systems*. Chichester, UK: Wiley; 1989:249-279.
9. Gabizon A. Selective tumor localization and improved therapeutic index of anthracyclines encapsulated in long-circulating liposomes. *Cancer Res* 1992;52:891-896.
10. Gabizon A, Uziely B, Kaufman B, Safra T, Catane R, Barenholz Y. A new generation of doxorubicin-loaded liposomes with improved localization in tumors: preclinical and clinical studies. In: Banzet P, Holland JF, Khayat D, Weil M, eds. *Cancer treatment. An update*. Paris: Springer-Verlag; 1994:820-822.
11. Bakker-Woudenberg IAJM, Lokense AF, ten Kate MT, Storm G. Enhanced localization of liposomes with prolonged blood circulation time in infected lung tissue. *Biochim Biophys Acta* 1992;1138:318-326.
12. Bakker-Woudenberg IAJM, Lokense AF, ten Kate MT, Mouton JW, Woodle MC, Storm G. Liposomes with prolonged blood circulation and selective localization in *Klebsiella pneumoniae*-infected lung tissue. *J Infect Dis* 1993;168:164-171.
13. Woodle MC, Lasic DD. Sterically stabilized liposomes. *Biochim Biophys Acta* 1992;1113:171-199.
14. Morgan JR, Williams LA, Howard CB. Technetium-labelled liposome imaging for deep-seated infection. *Br J Radiol* 1985;58:35-39.
15. O'Sullivan MM, Powell N, French AP, Williams KE, Morgan JR, Williams BD. Inflammatory joint disease: a comparison of liposome scanning, bone scanning and radiography. *Ann Rheum Dis* 1988;47:485-491.
16. Williams BD, O'Sullivan MM, Saggu GS, Williams KE, Williams LA, Morgan JR. Synovial accumulation of technetium-labelled liposomes in rheumatoid arthritis. *Ann Rheum Dis* 1987;46:314-318.
17. Love WG, Amos N, Kellaway IW, Williams BD. Specific accumulation of cholesterol-rich liposomes in the inflammatory tissue of rats with adjuvant arthritis. *Ann Rheum Dis* 1990;49:611-614.
18. Lang J, Vigo-Pelfrey C, Martin F. Liposomes composed of partially hydrogenated egg phosphatidylcholines: fatty acid composition, thermal phase behaviour and oxidative stability. *Chem Phys Lipids* 1990;53:91-101.
19. Woodle MC, Matthey KK, Newman MS, et al. Versatility in lipid compositions showing prolonged circulation with sterically stabilized liposomes. *Biochim Biophys Acta* 1992;1105:193-200.
20. Storm G, Van Bloois L, Brouwer M, Crommelin DJA. The interaction of cytostatic drugs with adsorbents in aqueous media. The potential implication for liposome preparation. *Biochim Biophys Acta* 1985;818:343-351.
21. Gabizon A, Huberty, Straubinger RM, Price DC, Papahadjopoulos D. An improved method for in vivo tracing and imaging of liposomes using a gallium-67-deferoxamine complex. *J Liposome Res* 1988;1:123-135.
22. Hnatowich DJ, Childs RL, Lanteigne D, Najafi A. The preparation of DTPA-coupled antibodies radiolabeled with metallic radionuclides: an improved method. *J Immunol Meth* 1983;65:147-157.
23. Oyen WJG, Claessens RAMJ, Van der Meer J, Corstens FHM. Biodistribution and kinetics of radiolabeled proteins in rats with focal infection. *J Nucl Med* 1992;33:338-394.
24. Tilcock C, Yap M, Szucs M, Utkhede D. PEG-coated lipid vesicles with encapsulated technetium-99m as blood-pool agents for nuclear medicine. *Nucl Med Biol* 1994;21:165-170.
25. Goins B, Klipper R, Rudolph AS, Cliff RO, Blumhardt R, Phillips WT. Biodistribution and imaging studies of technetium-99m-labeled liposomes in rats with focal infection. *J Nucl Med* 1993;34:2160-2168.
26. Allen TM, Hansen C, Rutledge J. Liposomes with prolonged circulation times: factors affecting uptake by reticuloendothelial and other tissues. *Biochim Biophys Acta* 1989;981:27-35.
27. Blume G, Cevec G. Liposomes for the sustained drug release in vivo. *Biochim Biophys Acta* 1990;1029:91-97.
28. Allen TM, Hansen C, Martin F, Redemann C, Yan-Young A. Liposomes containing synthetic lipid derivatives of polyethylene glycol show prolonged circulation half-lives in vivo. *Biochim Biophys Acta* 1991;1066:29-36.
29. Rubin RH, Fischman AJ, Needleman M, et al. Radiolabeled, nonspecific, polyclonal human immunoglobulin in the detection of focal inflammation by scintigraphy: comparison with gallium-67 citrate and technetium-99m-labeled albumin. *J Nucl Med* 1989;30:385-389.
30. Oyen WJG, Claessens RAMJ, van der Meer JWM, Corstens FHM. Detection of subacute infectious foci with indium-111-labeled autologous leukocytes and indium-111-labeled human nonspecific immunoglobulin G: a prospective comparative study. *J Nucl Med* 1991;32:1854-1860.
31. Crowe JH, Crowe LM, Carpenter JF, et al. Interactions of sugars with membranes. *Biochim Biophys Acta* 1988;947:367-384.
32. Lavender JP, Goldman JM, Arnot RN, Thakur ML. Kinetics of indium-111-labeled lymphocytes in normal subjects and patients with Hodgkin's disease. *Br Med J* 1977;2:797-799.
33. Coleman RE. Radiolabeled leukocytes. In: Freeman LM, Weissmann HS, eds. *Nuclear medicine annual 1982*. New York: Raven Press; 1982:119-141.